Available online at www.sciencedirect.com
SCIENCE DIRECT®
Surface Science 588 (2005) 61–70
SURFACE SCIENCE
www.elsevier.com/locate/susc

Relative stability of Si surfaces: A first-principles study

Guang-Hong Lu [a,b,*], Minghuang Huang [b], Martin Cuma [c], Feng Liu [b]

[a] School of Science, Beijing University of Aeronautics and Astronautics, Beijing 100083, China
[b] Department of Materials Science and Engineering, University of Utah, Salt Lake City, UT 84112, USA
[c] Center for High Performance Computing, University of Utah, Salt Lake City, UT 84112, USA

Received 1 March 2005; accepted for publication 11 May 2005
Available online 14 June 2005

Abstract

Surface energies of Si(0 0 1), (1 1 0), (1 1 1), and (1 1 3) surfaces with different reconstructions are calculated systematically using first-principles total-energy method. In order to quantitatively compare their relative stability, the surface energies of different surface orientations and their respective theoretical bulk atom energies are determined simultaneously by linear fitting slab supercell total energy as a function of the atom number in the slab. Equivalent computational parameters and convergence criteria are used for all calculations. Without considering entropy contribution, the relative stability of these Si surfaces with given reconstructions is shown, in decreasing order, from (1 1 1) to (0 0 1) and (1 1 3) at low temperature, and from (0 0 1), (1 1 3), (1 1 0), to (1 1 1) at high temperature.

Keywords: Si surfaces; Surface energy; Relative stability; First-principles calculation

1. Introduction

Surface energy is the most fundamental thermodynamic property of solid surfaces [1]. A solid surface can be created by cutting a crystal into half, and surfaces of different indices form when a crystal is cut along different orientations of the atomic plane. Because less number of atomic bonds are cut in creating a low-index surface, surface energy of a low-index surface is generally lower than that of a high-index surface. However, this general rule may fail sometimes when a large degree of surface reconstructions are involved, in particular for semiconductor surfaces.

Surface energy is difficult to measure directly. Experimentally, one way to determine the relative surface energy is by measuring an equilibrium crystal shape bounded by different surfaces (facets) combined with Wulff-theorem analysis [2]. In an equilibrium three-dimensional (3D) crystallite, the area of individual facets scales inversely with

* Corresponding author. Address: Department of Materials Science and Engineering, University of Utah, Salt Lake City, UT 84112, USA. Tel.: +1 801 581 6613; fax: +1 801 581 4816.
E-mail address: lgh@eng.utah.edu (G.-H. Lu).

0039-6028/$ - see front matter © 2005 Elsevier B.V. All rights reserved.
doi:10.1016/j.susc.2005.05.028

their surface energy. In addition to the relative surface energy, measurement of the absolute surface energy has also been attempted through two independent measurements on 3D and 2D equilibrium crystal shapes [3], but its accuracy remains to be improved. Theoretically, surface energy can be calculated using first-principles method.

The Si surface has been extensively studied both as the model system of semiconductor surfaces and because Si is the base material used in modern semiconductor industry. However, the relative stability of different Si surfaces has not yet been determined precisely and remains controversial. In a measurement of the equilibrium shape of Si void by He implantation, relative energies of Si{001}, {110}, {111}, and {113} surfaces have been determined, and {111} surface is shown to be the most stable Si surface [4,5]. In contrast, by using monocrystalline columns to obtain the equilibrium crystal shape of Si, {001} and {113} surfaces are suggested to be most stable [6].

Surface energies of various Si surfaces have also been calculated from first-principles. These include, for example, {001} [7–9], {111} [10–12], {110} [13], and {113} [14,15] surfaces. However, these calculations have been performed separately by different groups for individual surfaces. Consequently, a comparison between them is not reliable because the energies of these surfaces may differ only by a few meV, which is about the uncertainty inherent to a given first-principles calculation of surface energy. To obtain the relative stability of different Si surfaces, equivalent computational parameters and convergence criteria must be used for all the calculations to minimize systematic errors. One such attempt has been made by Stekolnikov et al. [16–18] who calculated the surface energies of Si{001}, {110}, {111}, and {113} surfaces.

A standard procedure for calculating surface energy is by the slab supercell technique, in which one needs to subtract bulk energy from total energy of slab supercell. However, the inaccurate bulk atom energy has been used to calculate surface energy, namely the same bulk atom energy obtained from a separate bulk calculation has been used for different surface orientations. Such a treatment can be used for comparing surface energy of different reconstructions for a given surface calculated with the same slab supercell. It is inappropriate, however, for comparing surface energy of different surface orientations. This is because such treatment will lead to a divergence of surface energy with increasing slab thickness due to the error in the bulk atom energy [19,20]. The proper way to derive surface energy and the corresponding bulk atom energy is by fitting total energy (E_T) of the slab supercell as a function of slab thickness or atom number (N) in the slab [19,20]. Such a procedure has to be applied to every surface orientation of slab calculation, because different bulk atom energies will be derived from different slabs due to difference in slab size and $\boldsymbol{k}$-point sampling, as absolute convergence is rarely achieved in the slab calculations.

Here, in order to determine the relative stability of Si surfaces more accurately, we apply such a procedure to calculate Si surface energies systematically using first-principles method. These include low-index surfaces of {001}, {110} and {111}, and high-index surface of {113}. To make a reliable comparison, we use equivalent parameter settings and convergence criteria for all the calculations to minimize the systematic errors, and the respective bulk Si atom energies for different surface orientations and slab sizes are correctly used to derive the surface energies by fitting the E_T–N curve. Although the calculations have been carried out at 0 K and thus the entropy contribution to the surface energy has not been considered, the present results will provide a good reference to assess the relative stability of Si surfaces at different temperatures.

2. Si surface reconstructions

Most semiconductor surfaces reconstruct driven by the desire to eliminate dangling bonds [1]. Si(001) surface represents a typical case where an atom-pairing mechanism works to remove one dangling bond per atom, forming dimers and doubling the periodicity along the [110] direction, resulting in a (2×1) reconstructed surface [21–23]. Furthermore, dimer buckling, a secondary effect to reduce the energy, leads to $p(2\times2)$ and $c(4\times2)$-

type of reconstructions [24–26]. Fig. 1 shows these reconstruction models. Fig. 1(a) shows ideal Si(0 0 1)-(1 × 1) surface with two dangling bonds on each surface atom. Fig. 1(b) shows (2 × 1) reconstruction, consisting of dimers that are arranged in parallel rows along the $[\bar{1}\,1\,0]$ direction. Only buckled dimers [noted as b(2 × 1)] are considered in our calculation. Fig. 1(c) and (d) illustrate, respectively, the p(2 × 2) and c(4 × 2) reconstructions, which are formed by alternation of buckled dimers with either in-phase or out-of-phase buckling, respectively.

At high temperature, Si(1 1 1) surface retains a unreconstructed (1 × 1) surface with one dangling bond on each surface atom; at low temperature, it transforms into a (7 × 7) reconstructed surface [1]. The transition temperature is about 850 °C and the transition is reversible. The low-temperature (7 × 7) phase is one of the most complex reconstructions that have been discovered for surfaces. It is described as the dimer-adatom-stacking-fault (DAS) structure [27,28]. The DAS model, as shown in Fig. 2, represents a complex interplay of different mechanisms between adatom, dimer, and stacking fault to eliminate dangling bonds. An as-cleaved Si(1 1 1) surface exhibits a (2 × 1) reconstruction, but it is metastable, converting irreversibly into the (7 × 7) structure after annealing at the elevated temperature [29]. So, we do not include it in our calculation.

Clean Si(1 1 0) surface transforms from a high-temperature (1 × 1) structure to a low-temperature (2 × 16) structure at a transition temperature about 750 °C. We calculate only surface energy of (1 × 1) reconstruction because the detailed structure of (2 × 16) reconstruction has not been completely clarified [13,30–34].

The Si(1 1 3) surface, oriented 25.2° from (0 0 1) to (1 1 1) face, is of much interest in spite of its high index. Si(1 1 3) has stable reconstructions [14,35]. It exhibits a (3 × 2) reconstruction at room temperature and undergoes a phase transition to (3 × 1) reconstruction at about 500 °C. Higher temperature (~570–750 °C) leads to (1 × 1) disordered phase. The bulk-terminated Si(1 1 3) surface has two types of atomic rows: one has two dangling bonds per atom similar to that of bulk-terminated (0 0 1) surface, and the other has one dangling bond per atom similar to that of bulk-terminated (1 1 1) surface, as indicated in Fig. 3(a). Fig. 3(b)–(e) shows different reconstruction models for Si(1 1 3) surface. Ranke proposed an adatom-dimer (AD)

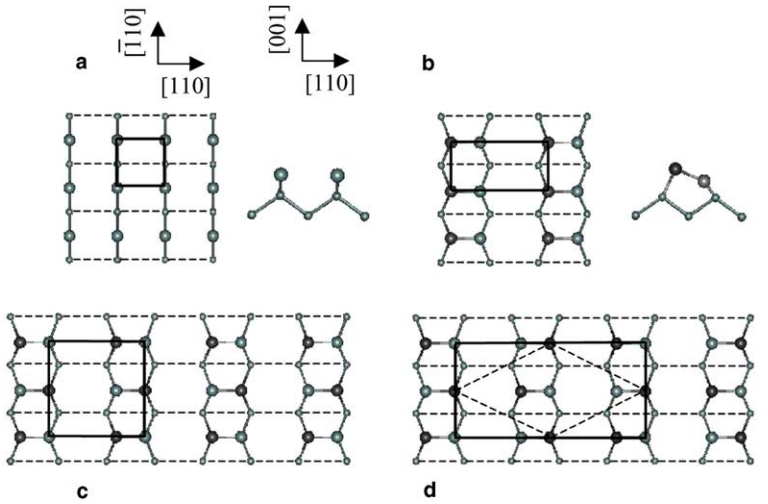

Fig. 1. Si(0 0 1) surface reconstruction models. The larger spheres represent the atoms at the first layer, in which the darker-grey-color ones indicate the atoms buckled up. Solid-line rectangles show the unit cells of respective case. (a) Ideal (1 × 1) surface, top view and side view. (b) b(2 × 1) reconstruction, top view and side view. (c) p(2 × 2) reconstruction. (d) c(4 × 2) reconstruction. The dashed-line rhombus indicates the primitive unit cell.

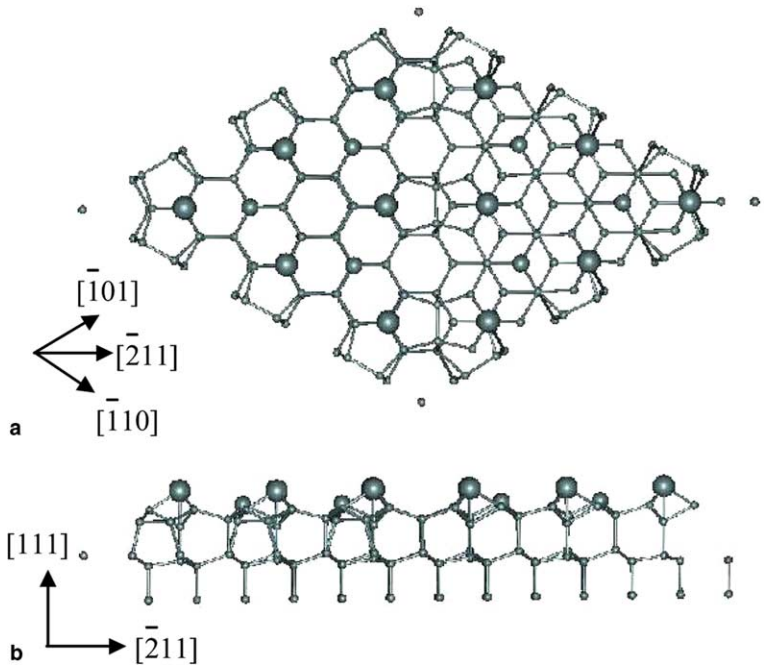

Fig. 2. Si(1 1 1)-(7 × 7) reconstructions—DAS model. (a) Top view (b) side view.

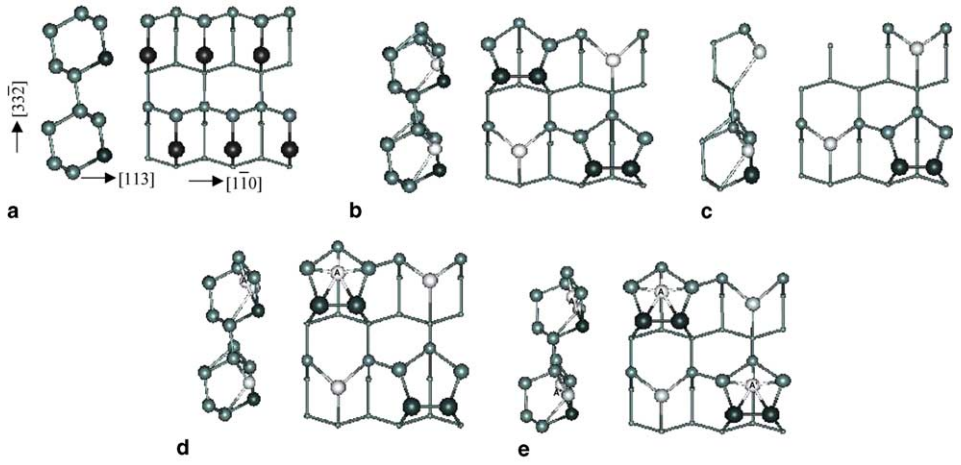

Fig. 3. Side view and top view of different Si(1 1 3) surface reconstruction models. Darker-grey-color spheres represent the atoms at the first layer. (a) Ideal (1 × 1) surface, (b) (3 × 1)-AD model, (c) (3 × 2)-AV model, (d) (3 × 2)-ADI model, (e) (3 × 1)-AI model.

model for the (3 × 1) reconstruction and adatom-void (AV) model for the (3 × 2) reconstruction [35]. In the AD model (Fig. 3(b)), every third (0 0 1)-like atom is removed and the remaining two atoms dimerize, resulting in formation of a pentagon containing this dimer. The removed atom is taken alternately from two lattices apart in the neighboring rows, leading to (3 × 1) reconstruction. This is equivalent to adding every two of three (0 0 1)-like atoms to the (1 1 1)-like surface forming

a dimer, so it is called AD model. If one of two the pentagons in the AD model is removed, the structure becomes a (3×2)-AV model, as shown in Fig. 3(c), in which strain is expected to be released around the adatoms. Dabrowski et al. proposed two different models for the (3×2) and (3×1) reconstructions [14]. They suggested adding a near-surface self-interstitial below one of the two pentagons in the AD model, forming an adatom-dimer-interstitial (ADI) model for (3×2) reconstruction, as shown in Fig. 3(d), and one each interstitial atom below both pentagons in the AD model, forming an adatom-interstitial (AI) model for (3×1) reconstruction, as shown in Fig. 3(e). They also suggested that the transition from (3×1) to (3×2) structure occurs through reducing one surface interstitial atom, and the AI reconstruction should exist in the (3×1) phase. However, so far the (3×1)-AI structure has not been confirmed experimentally [15]. We have compared energies for all these proposed reconstructions.

Wang et al. [36] purposed so-called 'puckered' Si(1 1 3)-(3×1) and (3×2) models based on Ranke's (3×1)-AD model. In both 'puckered' models, two (1 1 1)-like atoms in the pentagons of the (3×1)-AD model (Fig. 3(b)) are buckled significantly perpendicular to the surface. Puckered (3×1) and (3×2) reconstructions form if the neighboring pentagons in the (3×1)-AD model are buckled in the same or opposite way, respectively. According to the calculation of Stekolnikov et al. [17], the puckered (3×1) model has higher surface energy than the (3×1)-AI model, and the puckered (3×2) model has higher surface energy than the (3×2)-ADI model. Therefore, we exclude them from our calculations.

3. Methodology and computational details

We employ the pseudopotential plane wave total-energy method [37,38] based on the density functional theory within the local-density approximation [39–42]. The plane-wave kinetic energy cutoff is 12 Ry. For Brilliouin-zone sampling, a special grid of $\boldsymbol{k}$ points is chosen using the Monkhorst–Pack scheme [43]. We constructed ab initio semi-relativistic norm-conserving pseudopotential for Si [44,45]. We used theoretical Si lattice constant of 5.42 Å in all our surface energy calculations. All atoms are relaxed using the Hellman–Feynman scheme until all the forces are less than 0.01 eV/Å.

For all Si surfaces, we employ a slab supercell with the same reconstruction on the top and bottom of the supercell surface. In order to reduce the systematic error in comparing energies of different surfaces, we use the same computational setup as much as possible in all calculations. The thicknesses of the vacuum layers are 10 Å for all cases. Table 1 shows the surface size and corresponding $\boldsymbol{k}$-point sampling for various reconstruction models. The number of $\boldsymbol{k}$-points in surface Brilliouin zone (S.B.Z.) is chosen to scale closely with the surface unit cell size.

In calculating the surface energy E_s, one needs to subtract the bulk energy from the supercell total energy E_T, i.e.

$$E_s = (E_T - NE_b)/2A, \tag{1}$$

where E_b is the bulk atom energy, N is the number of atoms in the slab and A is the surface cell area.

Table 1
Surface cell size and $\boldsymbol{k}$-points sampling for various Si surfaces and reconstructions

Surface orientation	Reconstruction	Surface cell size (Å)	$\boldsymbol{k}$-points sampling in S.B.Z.
(0 0 1)	Ideal (1×1)	3.832×3.832	8×8
	Relax (1×1)	(orthorombic)	
	b(2×1)	3.832×7.664	8×4
		(orthorombic)	
	p(2×2)	7.664×7.664	4×4
		(orthorombic)	
	c(4×2)	7.664×15.327	4×2
		(orthorombic)	
(1 1 1)	Ideal (1×1)	3.832×3.832	8×8
	Relax (1×1)	(Hexagonal)	
	(7×7)-DAS	26.823×26.823	1×1
		(Hexagonal)	
(1 1 3)	Ideal (1×1)		
	Relax (1×1)		
	(3×2)-ADI	11.519×12.734	2×2
	(3×2)-AV	(orthorombic)	
	(3×1)-AD		
	(3×1)-AI		
(1 1 0)	Ideal (1×1)	3.832×5.429	8×4
	Relax (1×1)	(orthorombic)	

One method to obtain the bulk atom energy is to perform a separate bulk calculation; for example, using a two-atom diamond unit cell (we call this method as the '*bulk method*'). Although this method has been used to estimate the energy of a given surface orientation, it introduces systematic errors due to the different accuracies in the slab and bulk calculations [19,20].

To determine bulk atom energy accurately for a given size of a given surface orientation, we rewrite Eq. (1) as

$$E_T = NE_b + 2AE_s. \quad (2)$$

Obviously, the total energy E_T has a linear relation with atom number (N) in the slab because the surface energy E_s does not change with N if N (or slab thickness) is sufficiently large to eliminate interaction between the upper and lower surface. Therefore, as introduced by Gay et al. [19], we can calculate E_T as a function of N by increasing the atomic layers in the slab, and extract both the bulk atom energy and the surface energy by linear fitting of E_T–N curve (we call this method as the '*slab method*'). The slope and intercept of the fitted straight line are the bulk atom energy (E_b) and the surface energy contributed from the two surfaces ($2AE_s$), respectively.

Different bulk atom energy has to be fitted for every different surface orientations. However, because the bulk atom energy is the same for a given surface orientation of different surface reconstructions calculated from the same supercell slab, we need to fit the bulk atom energy for a given surface orientation of slab only once to save the computational time.

4. Results and discussion

4.1. Bulk atom energy

We use slab thickness of 16–22 layers (20.32–28.45 Å) for (0 0 1) surface, 11–17 layers (19.16–30.65 Å) for (1 1 0) surface, 14–20 layers (19.55–28.94 Å) for (1 1 1) surface, and 24–30 layers (18.38–23.28 Å) for (1 1 3) surface to fit the E_T–N curve to accurately determine the bulk atom energy. The results are shown in Table 2, in comparison with the bulk atom energy determined by the bulk method (−5.993 eV). It clearly shows that the bulk atom energy obtained from the slab method depends on both surface orientation and slab size, and they all differ from that obtained from the bulk method. Using the bulk atom energy determined by the bulk method will cause a divergence of surface energy with increasing slab thickness, and introduce different errors in different surface orientations. This makes the comparison of stability of different surface orientations unreliable.

Theoretically if number of atoms N (or slab thickness) are large enough, surface energy E_s will not change with N and converge to a constant value. However, if the bulk atom energy E_b calculated from the bulk method is not equal to the value from the slab method, E_s will diverge. Fig. 4 shows the surface energy of Si(1 1 1)-(1 × 1) surface as a function of the number of atomic layers calculated by the slab and bulk method, respectively. Initially, surface energy by both methods increases with the increase of the number of atomic layers. Beyond 12 layers of slab thickness, surface energy by the slab method converges to a constant value, while surface energy by the bulk method diverges. In principle, the bulk method can never give a unique surface energy value, because the result depends on the slab thickness one would use. This error has been overlooked in some of the previous calculations.

4.2. Surface energies and relative stability

Table 3 shows the calculated results of surface energies for the various Si surfaces. The surface energies determine the relative stability of different

Table 2
Bulk atom energies obtained by linear fitting of E_T–N curve according to Eq. (2)

Surface orientation or reconstruction	(0 0 1)	(1 1 0)	(1 1 1)-(1 × 1)	(1 1 1)-(7 × 7)	(1 1 3)	Bulk method
Bulk atom energy (eV)	−6.000	−5.999	−6.020	−5.996	−6.010	−5.993

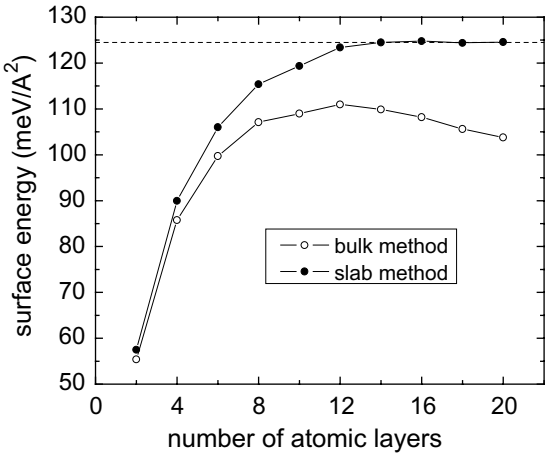

Fig. 4. Surface energy as a function of number of atomic layers for Si(1 1 1)-(1 × 1) surface. Solid and blank circles represent surface energy from the slab method and the bulk method, respectively.

Si surfaces. Because surfaces adopt different reconstructions at different temperatures, we assess their relative stability at high and low temperatures separately by calculating the surface energies of high- and low-temperature structures, respectively. It should be noted that the present calculations were carried out at 0 K, so the calculated surface energy is the internal energy U. At finite temperature, one must take into account the entropy contribution and use surface free energy $F = U - TS$ instead of U, where T and S are temperature and entropy, respectively. Therefore, the relative stability, we discuss here does not include the entropy contribution. Furthermore, at high temperature, surfaces may disorder without perfect reconstructed surface structures, making the theoretical calculations impossible. Nevertheless, if we consider the entropy contribution is small for well-ordered surface structures, we may still make a qualitative comparison of the relative stability between different high-temperature surface reconstructions (if they can exist), which may provide some useful theoretical reference in understanding the experimental assessment on the relative surface stability at high temperature.

Table 3
The surface energies (meV/Å^2) of different Si surface orientations calculated by the slab method[a]

Surface orientation	Surface reconstruction	Surface energy	Surface energy (Refs. [16–18])
(0 0 1)	Ideal (1 × 1)	161.2	149.1
	Relaxed (1 × 1)	147.1	149.1
	b(2 × 1)	94.1	90.5
	p(2 × 2)	92.0	–
	c(4 × 2)	91.9	88.0
(1 1 1)	Ideal (1 × 1)	139.1	113.6
	Relaxed (1 × 1)	124.5	108.6
	(7 × 7)-DAS	88.6	84.9
(1 1 3)	Ideal (1 × 1)	145.8	137.9
	Relaxed (1 × 1)	113.5	115.5
	(3 × 2)-AV	106.1	–
	(3 × 2)-ADI	94.8	87.4
	(3 × 1)-AD	98.9	93.0
	(3 × 1)-AI	96.3	90.5
(1 1 0)	Ideal (1 × 1)	130.5	127.3
	Relaxed (1 × 1)	109.5	106.1

[a] Surface energies from Refs. [16–18] are also presented for comparison.

The high-temperature structure of Si(0 0 1) is still controversial. It may be a dynamic mixture of all of the possible reconstructions or one kind of reconstruction. Nevertheless, the surface energy falls in the range from 92 to 94 meV/Å^2 for these different reconstructions. Si(1 1 3) surface has (3 × 1) reconstruction at high temperature, whose surface energy is 96.3 meV/Å^2 for the (3 × 1)-AI model, and 98.9 meV/Å^2 for the (3 × 1)-AD model. Because there are no reconstructions for (1 1 1) and (1 1 0) at high temperature, we take their energies from the non-reconstructed surface, which are 124.5 and 109.5 meV/Å^2, respectively. Therefore the relative stability of these Si surfaces from high to low at high temperature is (0 0 1), (1 1 3), (1 1 0), and (1 1 1), regardless of it we take (3 × 1)-AI or -AD model for the (1 1 3) surface.

At low temperature, Si(1 1 1) surface exhibits (7 × 7)-DAS reconstruction, while (1 1 3) surface shows (3 × 2)-ADI reconstruction. Their surface energies are 88.6 and 94.8 meV/Å^2, respectively. The surface energy of Si(0 0 1) at low temperature should be ~92 meV/Å^2 for p-(2 × 2) and/or c(4 × 2) structures at very low temperature, and 92–94 meV/Å^2 at room temperature. Consequently, surface energy of Si(0 0 1) and (1 1 3) is about

degenerate within the computational accuracy. The surface energy of Si(1 1 3) is much higher than those of (1 1 1) surfaces, and the (1 1 1) surface has the lowest surface energy among them. Therefore, the relative stability of these Si surfaces from high to low at low temperature are (1 1 1) and (0 0 1), (1 1 3). Also, it is shown that (3×2)-AV model is not an energy-favorable one though it is believed that this structure can relieve the strain [35]. We have not calculated the surface energy of Si(1 1 0) surface at low temperature. However, Si(1 1 0) is generally considered as a high-energy surface compared to (0 0 1) and (1 1 1).

For a given surface orientation, the relative surface energies of different reconstructions calculated by the different groups show the same trend with difference absolute values, using either slab or bulk method. For example, for Si(0 0 1), $p(2\times2)$ and $c(4\times2)$ reconstructions have the lower surface energy than $b(2\times1)$, and the surface energy of $c(4\times2)$ is the lowest. The surface energies of different Si(1 1 3) reconstructions calculated by Dabrowski et al. [14] are 111, 97, 99, 99 meV/Å^2 for (3×2)-AV, (3×2)-ADI, (3×1)-AD, and (3×1)-AI, respectively. While the values calculated by Laracuente et al. [15] are 93, 97, 95 for (3×2)-ADI, (3×1)-AD, and (3×1)-AI reconstructions, respectively. Both have the same trend as the present calculations. Therefore, the bulk method is applicable for comparing the relative stability of different reconstructions for a given surface orientation, provided they are calculated with the same slab thickness and surface cell size.

However, it is unreliable to compare the relative stability between different surface orientations using the calculation results from different groups, especially because of the possible error in bulk atom energy. For example, our calculations show that the slab method predicts the Si(1 1 1) surface to be more stable than (1 1 3) at low temperature, but the bulk method would predict the two surfaces to be degenerate.

4.3. Comparison with the experimental results

In the experiments, the surface free energy was measured at high temperature in order to obtain the equilibrium crystal shape and thus includes entropy contribution. Also, as we mentioned above, the surface may transform to disordered structure at high temperature. Therefore, the calculated results might not be directly comparable to experiments. However, if we consider the entropy contribution is small for well-ordered surface structures and assuming the surface reconstruction exists at high temperature, we may still theoretically compare their relative stability.

It is very difficult to measure the absolute surface energy by experiments. Only the relative surface energies of certain Si surfaces have been measured [4–6]. These results are summarized in Table 4. Eaglesham et al. [4] showed that the surface energies of Si {1 0 0}, {1 1 3} and {1 1 0} are 1.11, 1.13, 1.16 times of that of {1 1 1}, respectively, and therefore {1 1 1} is the most stable surface. Follstaedt [5] showed that the surface energies of Si{0 0 1} and {1 1 0} planes are 1.09 and 1.07 times of that of {1 1 1} planes, indicating also that {1 1 1} is the most stable surface. In contrast, Bermond et al. [6] showed that the surface energies of {0 0 1} and {1 1 3} are, respectively, 3% and 2% lower than that of {1 1 1} surface, indicating that Si{0 0 1} and {1 1 3} surfaces are more stable than {1 1 1}.

The present calculations show that assuming the surfaces are reconstructed as shown in Table 4 at high temperature, the surface energy of (1 1 1) is the highest, and the surface energies of (0 0 1), (1 1 3) and (1 1 0) are 75%, 78% and 86% of that of (1 1 1) surface, respectively, which indicates that (0 0 1) and (1 1 3) surfaces are more stable. Thus, our idealized theoretical order is more

Table 4
Surface energies of Si{0 0 1}, {1 1 3} and {1 1 0} in comparison with that of {1 1 1} from the experiments and the present calculations

		{0 0 1}	{1 1 3}	{1 1 0}
	Ref. [4]	1.11	1.13	1.16
	Ref. [5]	1.09	1.07	–
	Ref. [6]	0.97	0.98	–
Present calculation	High temperature	~0.75	0.78	0.86
	Low temperature	1.04–1.06	1.07	–

consistent with the experimental results of Bermond et al. [6].

Recently an attempt to determine the absolute surface energy of Si has also been made based on two independent measurements on 3D and 2D crystal equilibrium shapes by the analysis of the thermal fluctuation of an isolated step [3]. The surface energy of Si{1 1 1} at 1372 K is determined to be ranging from 36.8 to 51.2 meV/Å^2. Future theoretical calculation of surface free energy is needed to make a comparison.

5. Summary

Surface energies of Si(0 0 1), (1 1 0), (1 1 1), and (1 1 3) are calculated using first-principles total-energy method in order to determine the relative stability of these surfaces. Various reconstructions are considered for these surfaces. In order to obtain the reliable surface energy comparison, in addition to using equivalent computational parameters and convergence criteria for all calculations, we determine Si bulk atom energies for different surface orientations by linear fitting of slab supercell total energy as a function of atom number in the slab. Without considering entropy contribution, the relative stability of these Si surfaces from high to low is (1 1 1) to (0 0 1) and (1 1 3) at low temperature, and (0 0 1), (1 1 3), (1 1 0), and (1 1 1) at high temperature, assuming the surfaces are ideally reconstructed. Si(1 1 3) is a stable surface for its given reconstructions at both high and low temperature in spite of its high index.

Acknowledgements

This research is supported by US Department of Energy (DOE). G.-H. Lu acknowledges the support from National Natural Science Foundation of China (NSFC) and also thanks Dr. Wenqing Zhang for helpful discussions. The calculations were performed on IBM SP RS/6000 at NERSC and ORNL, Cray T3E at Pittsburgh Supercomputing Center (PSC) and AMD Opteron cluster in Center for High Performance Computing (CHPC) in University of Utah.

References

[1] F. Liu, M. Hohage, M.G. Lagally, Encyclopedia of Applied Physics, Wiley-VCH Verlag GmbH, London, 1999, p. 321.
[2] G. Wulff, Z. Kristallogr. 34 (1901) 449.
[3] J.J. Métois, P. Müller, Surf. Sci. 548 (2004) 13.
[4] D.J. Eaglesham, A.E. White, L.C. Feldman, N. Moriya, D.C. Jacobson, Phys. Rev. Lett. 70 (1993) 1643.
[5] D.M. Follstaedt, Appl. Phys. Lett. 62 (1993) 1116.
[6] J.M. Bermond, J.J. Métois, X. Egéa, F. Floret, Surf. Sci. 330 (1995) 48.
[7] Z. Zhu, N. Shima, M. Tsukada, Phys. Rev. B 40 (1989) 11868.
[8] F. Liu, M.G. Lagally, Phys. Rev. Lett. 76 (1996) 3156.
[9] S.C. Erwin, A.A. Baski, L.J. Whitman, Phys. Rev. Lett. 77 (1996) 687.
[10] D. Vanderbilt, Phys. Rev. Lett. 59 (1987) 1456.
[11] R.D. Meade, D. Vanderbilt, Phys. Rev. B 40 (1989) 3905.
[12] K.D. Brommer, M. Needels, B.E. Larson, J.D. Joannopoulos, Phys. Rev. Lett. 68 (1992) 1355.
[13] N. Takeuchi, Surf. Sci. 494 (2001) 21.
[14] J. Dabrowski, H.-J. Müssig, G. Wolff, Phys. Rev. Lett. 73 (1994) 1660.
[15] A. Laracuente, S.C. Erwin, L.J. Whitman, Phys. Rev. Lett. 81 (1998) 5177.
[16] A.A. Stekolnikov, J. Furthmüller, F. Bechstedt, Phys. Rev. B 65 (2002) 115318.
[17] A.A. Stekolnikov, J. Furthmüller, F. Bechstedt, Phys. Rev. B 67 (2003) 195332.
[18] A.A. Stekolnikov, J. Furthmüller, F. Bechstedt, Phys. Rev. B 68 (2003) 205306.
[19] J.G. Gay, J.R. Smith, R. Richter, F.J. Arlinghaus, R.H. Wagoner, J. Vac. Sci. Technol. A 2 (1983) 931.
[20] V. Fiorentini, M. Methfessel, J. Phys.: Condens. Matter 8 (1996) 6525.
[21] R.E. Schlier, H.E. Farnsworth, J. Chem. Phys. 30 (1985) 917.
[22] R.M. Tromp, R.J. Hamers, J.E. Demuth, Phys. Rev. Lett. 55 (1985) 1303.
[23] R.J. Hamers, R.M. Tromp, J.E. Demuth, Phys. Rev. B 34 (1986) 5343.
[24] D.J. Chadi, Phys. Rev. Lett. 43 (1979) 43.
[25] T. Tabata, T. Aruga, Y. Murata, Surf. Sci. 179 (1987) L63.
[26] A. Ramstad, G. Brocks, P.J. Kelly, Phys. Rev. B 51 (1995) 14504.
[27] K. Takayanagi, Y. Tanishiro, M. Takahashi, S. Takahashi, J. Vac. Sci. Technol. A3 (1985) 1502.
[28] K. Takayanagi, Y. Tanishiro, M. Takahashi, S. Takahashi, Surf. Sci. 164 (1985) 367.
[29] J.J. Lander, G.W. Gobeli, J. Morrison, J. Appl. Phys. 34 (1963) 2298.
[30] Y. Yamamoto, S. Kitamura, M. Iwatsuki, Jpn. J. Appl. Phys. 31 (1992) L635.
[31] Y. Yamamoto, Phys. Rev. B 50 (1994) 8534.
[32] W.E. Packard, J.D. Dow, Phys. Rev. B 55 (1997) 15643.

[33] M. Menon, N.N. Lathiotakis, A.N. Andriotis, Phys. Rev. B 56 (1997) 1412.
[34] T. An, M. Yoshimura, I. Ono, K. Ueda, Phys. Rev. B 61 (2000) 3006.
[35] W. Ranke, Phys. Rev. B 41 (1990) 5243.
[36] J. Wang, A.P. Horsfield, D.G. Pettifor, M.C. Payne, Phys. Rev. B 54 (1996) 13744.
[37] M. Huang, M. Cuma, F. Liu, Phys. Rev. Lett. 90 (2003) 256101.
[38] G.-H. Lu, S. Deng, T. Wang, M. Kohyama, R. Yamamoto, Phys. Rev. B 69 (2004) 134106.
[39] G.P. Hohenberg, W. Kohn, Phys. Rev. B 136 (1964) 864.
[40] W. Kohn, L.J. Sham, Phys. Rev. A 140 (1965) 1133.
[41] D.M. Ceperley, B.J. Alder, Phys. Rev. Lett. 45 (1980) 566.
[42] J.P. Perdew, A. Zunger, Phys. Rev. B 23 (1981) 5048.
[43] H.J. Monkhorst, J.D. Pack, Phys. Rev. B 13 (1976) 5188.
[44] D.R. Hamann, M. Schlüter, C. Chiang, Phys. Rev. Lett. 43 (1979) 1494.
[45] G.B. Bachelet, D.R. Hamann, M. Schlüter, Phys. Rev. B 26 (1982) 4199.